NASA Technical Memorandum 86310

NASA-TM-86310 19850002831

TENSILE STRENGTH OF COMPOSITE SHEETS WITH UNIDIRECTIONAL STRINGERS AND CRACK-LIKE DAMAGE - A BRIEF REPORT

C. C. POE, JR.

SEPTEMBER 1984

NASA
National Aeronautics and
Space Administration

Langley Research Center
Hampton, Virginia 23665

Summary

The purpose of this investigation was to determine the residual strength of composite sheets with bonded composite stringers loaded in tension. This report summarizes the results.

About 50 graphite/epoxy composite panels with crack-like slots were monotonically loaded in tension to failure. Both sheet layup and stringer configuration were varied. The tests indicate that the composite panels have considerable damage tolerance. The stringers arrested cracks that ran from the crack-like slots, and the residual strengths were considerably greater than those of unstiffened composite sheets.

A stress-intensity factor analysis was developed to predict the failing strains of the stiffened panels. Using the analysis, a single design curve was produced for composite sheets with bonded stringers of any configuration.

INTRODUCTION

The damage tolerance characteristics of metal tension panels with riveted and bonded stringers are well known. The stringers arrest unstable cracks and retard the propagation of fatigue cracks. Residual strengths and fatigue lives are considerably greater than those of unstiffened or integrally stiffened sheets.

This report summarizes the results of an investigation to determine the damage tolerance of composite sheets with bonded composite stringers loaded in tension. Cracks in composites do not readily propagate in fatigue, at least not through fibers. Moreover, the residual strength of notched composites is sometimes even increased by fatigue loading. Therefore, the residual strength aspect of damage tolerance, and not fatigue crack propagation, was investigated.

To this end, about 50 graphite/epoxy composite panels with two sheet layups and several stringer configurations were monotonically loaded in tension to failure. Crack-like slots were cut in the middle of the panels to simulate damage.

A stress-intensity factor analysis was developed to predict the failing strains of the stiffened panels. Using the analysis, a single design curve was produced for composite sheets with bonded stringers of any configuration.

SYMBOLS

a	half-length of crack, in.
a_o	initial half-length of crack, in.
E	Young's modulus, psi

F_{tu} uncracked tensile strength, psi

K_Q critical stress-intensity factor or fracture toughness, psi-in.$^{1/2}$

ℓ length of disbond, in.

N number of plies

Q_c general fracture toughness parameter, in.$^{1/2}$

S applied stress, psi

SCF strain concentration factor

t thickness, in.

W_a distance between stringer edges, in.

W_{st} width of stringers, in.

α stringer stiffness ratio, $\alpha = (tE)_{st}/(tE)_{sh}$

α^* stringer stiffness ratio for maximum stringer effectiveness

γ exponential coefficient

ε strain

ε_c strain associated with critical stress-intensity factor

ε_{ci} failing strain of unstiffened sheet

ε_{cu} failing strain of stiffened sheet

ε_{tu} strain associated with F_{tu}

ε_{tuf} failing strain of fiber

μ stiffness ratio, $\mu = (WtE)_{st}/[(WtE)_{st}+(WtE)_{sh}]$

ν Poisson's ratio

ξ layup parameter

Subscripts:

1	refers to stringer region of monolithic sheet in shear-lag analysis
N	factor indicating how many times plies are repeated in a layup
sh	refers to sheet
st	refers to stringers
S	indicates symmetric layup
T	indicates total number of plies
x,y	Cartesian coordinates

The following notation is used to prescribe the laminate orientation or layup. Ply angles are separated by a slash and listed in the order of layup. A numerical subscript on the ply angle denotes how many consecutive plies are at that angle. The subscript S outside of the parentheses that enclose the listing denotes symmetric. A numerical factor of S denotes how many times the plies within the parentheses are repeated. For example, $(0_2/\pm45)_{2S}$ means (0/0/45/-45/0/0/45/-45/-45/45/0/0/-45/45/0/0).

CONFIGURATION OF STIFFENED PANELS

The configuration of the panels is shown in figure 1. The panels were 12 inches wide and 24 inches long between the grips of the testing machine. The sheet and stringers were made with graphite/epoxy prepreg tape. The graphite fibers were T300 made by Union Carbide and the epoxy was 5208 made by Narmco Materials Inc. The sheet and stringers were cocured with film adhesive added to the stringer-sheet interface. The sheets were 16 plies thick and made with $(45/0/-45/90)_{2S}$ and $(45/0/-45/0)_{2S}$ layups. The stringers were unidirectional and had various widths and thicknesses. The values of stringer area were chosen such that the ratio of stringer stiffness to panel stiffness μ was 0.3, 0.5, and 0.7. Consequently, for a given stiffness ratio, the stringers were thicker for the stiffer $(45/0/-45/0)_{2S}$ sheets than for the $(45/0/-45/90)_{2S}$ sheets.

Three or six panels were made of each type. The panels were loaded in tension at the ends to produce uniform axial strain parallel to the stringers. Load and not displacement was controlled. Crack-like slots of various lengths were machined into the sheets at the middle of the panels to represent damage.

TEST RESULTS FOR $(45/0/-45/90)_{2S}$ PANELS WITH $\mu = 0.7$

First, some typical test results are presented to show how the cracks initiated and were arrested. Strain versus crack-tip position is shown in figure 2 for the three $(45/0/-45/90)_{2S}$ panels with $\mu = 0.7$. As the panels were loaded, cracks initiated and ran from the slot ends at strains that correspond to the failing strains of unstiffened sheets. (The failing-strain curve without

stringers is associated with initial crack length or slot length, not final length. Thus, the strains at instability actually agree better with the curve than indicated.) For the shortest slot, the crack was not arrested. But for the longest slots, the stringers arrested the cracks and loading was continued. Eventually, the sheet and stringers appeared to fail simultaneously at a strain considerably larger than that for a sheet without stringers. This behavior is typical of all the panels. Usually, when cracks were not arrested, failing strains were slightly less than (within 10 percent) or equal to those when cracks were arrested.

During each test, crack-opening displacements were measured continuously, and loading was halted numerous times to make radiographs of the crack tips. An opaque dye (zinc iodide) was used to enhance the visibility of matrix damage. The radiographs and crack-opening displacements were used to estimate the crack tip positions plotted in figure 2. The last radiograph of panel C, which was made at a strain corresponding to 97 percent of the failing strain, is also shown in figure 2. (The last radiograph of panel B has the same appearance as that of panel C.) The two dark rectangular regions are the stringers. (Strain gages and wires can also be seen.) The even darker regions at the ends of the crack are disbonds between the sheet and stringers. (Actually, the disbond is between the two outermost plies of the sheet.) Probably large shear stresses were the principal cause of the disbonds. The radiograph indicates that the arrested crack ran under the stringers about 1/3 inch. Usually the cracks extended to the disbond fronts.

TEST RESULTS FOR $(45/0/-45/90)_{2S}$ PANELS WITH $\mu = 0.5$

Strain versus crack-tip position is shown in figure 3 for three of the panels with $\mu = 0.5$ and stringers of different thicknesses and widths. The initiation and arrest of cracks is similar to that in figure 2. The last radiographs are also shown in figure 3. They were made within 5 to 10 percent of the failing load. For lack of space, only one crack tip is shown. (Both crack tips had virtually the same position and appearance.) For the thinnest stringers, panel A, the crack arrested at the inside edge of the stringer. But, for the thicker stringers, panels B and C, the stringers disbonded locally, and the cracks ran beneath the stringers. For the thickest stringers, panel C, the crack ran to a point slightly beyond the outside edge of the stringer. The shear stresses that caused the disbonds are larger for thicker stringers. The large disbonds like that in panel C of figure 3 did not always occur in panels with very thick stringers. On the other hand, large disbonds never occurred in panels with thin stringers. The size of disbonds often varied quite a bit among like panels with thick stringers. The variations seemed somewhat random as though they were caused by variations in interface strength.

ANALYSIS FOR BONDED STRINGERS

The stress-intensity factor has been determined for a cracked sheet with bonded and partially disbonded stringers (ref. 1). The stiffnesses of the stringers and adhesive were taken into account. The stringer was assumed to act along its centerline, that is, to have no width. For a critical value of the stress-intensity factor, the corresponding strain was calculated and plotted

against half-length of crack in figure 4. Results are shown with and without stringers for different values of stringer and adhesive stiffness and disbond length. Because the stringers reduce the stress-intensity factor, the critical-strain curves with stringers are above that without stringers. They have high peaks when the crack tip is just beyond the stringer. The curve is lower with a disbond ($\ell > 0$). If the stringers were completely disbonded, the curves with and without stringers would be the same. The curve is higher for a stiffer adhesive and stiffer stringers. For a rigid adhesive and $\ell=0$, the critical strain would go to infinity for the crack tip at the stringer centerline, regardless of the stringer stiffness.

The critical strain is replotted against half-length of crack for different disbond lengths in figure 5. For an initial half-length of crack a_o, the results indicate that the crack would run at a far-field strain of ε_{ci} and be arrested at the stringer if $\varepsilon_{ci} \leq \varepsilon_{cu}$. (A small dynamic amplification of crack-tip stresses may require ε_{ci} to be even less for arrest.) Upon increasing the load further, the arrested crack would run at ε_{cu}. Short cracks, where $\varepsilon_{ci} > \varepsilon_{cu}$, would not be arrested, and failing strains would be greater than ε_{cu}. Thus, for arrested cracks, the failing strain ε_{cu} would be given by the peak value of ε_c, which decreases with disbond length and increases with adhesive and stringer stiffness. Also, for a given adhesive stiffness, stringer stiffness, and disbond length, ε_{cu} is independent of a_o. For short cracks that are not arrested, $\varepsilon_{cu} = \varepsilon_{ci}$. Typically, the data followed this trend.

Without dynamic effects, panels without arrested cracks (short slots) should fail at strains greater than or equal to those of panels with arrested cracks. Because the lengths of the shortest slots were chosen to give failing strains on the verge of arrest, failing strains of panels without arrested cracks were usually close to those of panels with arrested cracks. However, as noted previously, the failing strains of panels without arrested cracks were usually 90 to 100 percent of those of panels with arrested cracks. Thus, the dynamic effect was less than 10 percent.

Although this analysis gives insight into how the failing strains of stiffened panels are affected by configuration and material, it would not give very accurate predictions of failing strain. The stress-intensity factor for the sheet would be greatly underestimated for wide stringers when there is little or no disbonding because the stringers are assumed to act (or to be concentrated) at their centerlines. Predictions would be more accurate if the disbond was long compared to stringer width. But, only a few panels with very thick, narrow stringers had long disbonds.

Furthermore, the results in figure 5 only account for failure of the sheet. Thin well-bonded stringers would also have large local stresses when the crack tip approaches. Thus, the stringers could fail as the crack tip approaches or between the times the crack arrests and and runs again. Then, the failing strain of the panel would be below that given by the peaks of the curves for sheet failure in figure 5. In tests of two identical panels with 8-ply-thick stringers and the same slot length, the crack was arrested in one panel but not

in the other. This difference was probably caused by a difference between the strengths of the stringer-sheet interfaces or between interlamina strengths of the sheet. (Recall that the disbond beneath the stringers usually occurred between the first two plies of the sheet and not at the actual stringer-sheet interface.) A weak interface would disbond and reduce the local stresses in the stringers, but a strong interface would not. Because of the thin stringers, the interface strength for these panels was probably marginal, and one disbonded and one did not. The panel with the arrested crack eventually failed at a strain 1.38 times that of the panel with the crack that did not arrest. Thus, interface strength may have a significant effect on the failing strain of a stiffened panel with stringers that have small Et. (The local stresses in the stringers and the interface shear stress, like the stress-intensity factor for the sheet, are not predicted accurately by the analysis in reference 1.)

SHEAR-LAG ANALYSIS

A shear-lag analysis was made of a stiffened panel treating the stringers as monolithic regions of the sheet. See figure 6. The sheet and stringers have Young's moduli E_{sh} and E_{st} in the loading direction and thicknesses t_{sh} and t_{st}, respectively. Within the region of the stringers, the stringers and sheet are assumed to act in parallel, and the stiffness is given by $(Et)_1 = (Et)_{sh} + (Et)_{st}$. The crack was assumed to extend completely across the sheet between stringers as though it was arrested.

Typical results are shown in figure 6. The logarithm of the strain-concentration factor (SCF) is plotted against the logarithm of an effective crack length $W_a(Et)_{sh}/(Et)_1$. The SCF is the ratio of the strain at the crack tip to the far-field strain. (The shear-lag analysis gives a finite crack-tip strain.) For $W_a = 0$, SCF = 1 as required, and for a large effective crack length, SCF $\propto [W_a(Et)_{sh}/(Et)_1]^{1/2}$. For an unstiffened sheet, $W_a(Et)_{sh}/(Et)_1 = W_a$, and the shear-lag and stress-intensity factor analyses give similar results. This similarity suggests that a stress-intensity factor can be synthesized using the shear-lag results.

For riveted stringers, which are attached to the sheet at essentially discreet points, the stress-intensity factor decreases with stringer area (ref. 2). However, for fully bonded stringers, the shear-lag analysis indicates that stringer width W_{st} has little effect on the SCF as long as W_{st} is large compared to a characteristic dimension of the order of fiber spacing. Thus, for fully bonded stringers, the thickness is more important than the area. However, with very large disbonds ($\ell \approx W_{st}$), W_{st} should also be important.

SYNTHESIZED STRESS-INTENSITY FACTOR

Without stringers, the critical value of the stress-intensity factor K_Q is given by

$$K_Q = S_{sh}[\pi a+(K_Q/F_{tu})^2]^{1/2} \quad (1)$$

where S_{sh} is the stress at failure applied to the sheet and F_{tu} is the uncracked strength of the sheet. (Note that the stress applied to the stringer region in figure 6 is $S_{sh}E_1/E_{sh}$.) The term $(K_Q/F_{tu})^2$ was included in equation (1) to give $S_{sh} = F_{tu}$ when $a = 0$ as required. For a state of uniaxial stress, $S_{sh} = E_{sh}\varepsilon_c$ and $F_{tu} = E_{sh}\varepsilon_{tu}$. Substituting these expressions into equation (1) for stresses and solving for $\varepsilon_{tu}/\varepsilon_c$ gives

$$\varepsilon_{tu}/\varepsilon_c = [1+\pi a(\varepsilon_{tu}E_{sh}/K_Q)^2]^{1/2} \quad (2)$$

The left-hand side of equation (2) is equivalent to the SCF in figure 6.

Replacing a in equation (2) by $\frac{1}{2}W_a(Et)_{sh}/(Et)_1$ (the effective crack length from the shear-lag results) and defining $\alpha = (Et)_{st}/(Et)_{sh}$, gives

$$\varepsilon_{tu}/\varepsilon_c = (\varepsilon_{tu}E_{sh}/K_Q)[(\varepsilon_{tu}E_{sh}/K_Q)^2+\tfrac{1}{2}\pi W_a/(1+\alpha)]^{1/2} \quad (3)$$

For small and large effective crack lengths, equation (3) models the essential features of the shear-lag results in figure 6; that is, for $W_a = 0$, SCF = 1, and, for large W_a, SCF $\propto [W_a/(1+\alpha)]^{1/2}$.

failing strains were predicted with equation (3) and compared with the test data. The values of K_Q, the elastic constants, and ε_{tu} used to make the calculations are given in reference 3 as "Manufacturer A" material.

FAILING STRAIN VERSUS STRINGER THICKNESS

failing strains are plotted against stringer thickness in figure 7 for panels in which cracks were arrested. (failing strains of panels without arrested cracks are not plotted. As noted previously, they should be larger than those of like panels with arrested cracks, but were usually a little smaller due to dynamic effects.) The panels had 1-inch-wide stringers and both $(45/0/-45/90)_{2S}$ and $(45/0/-45/0)_{2S}$ sheets. Predicted curves are plotted for comparison. For stringer thicknesses less than 20 or 30 plies, depending on sheet layup, the differences between measured and predicted failing strains are within the scatter among like specimens. For thicker stringers, equation (3) overestimates the failing strain. This discrepancy is probably due to out-of-plane effects, which give rise to strain gradients through the thickness. These strain gradients are not modeled in the plane analysis. They increase the membrane components of the crack-tip stresses by reducing the effective stiffness of the stringers, and they give rise to bending components. Both would reduce the failing strain of the panels.

Initially, three panels were made of each type. Some months later, an additional three panels of some types were made with stronger ends to avoid the possibility of failure in the grips. In some cases, both groups of like panels failed in the test section. Although the failing strains should have been equal, they were noticeably different. These discrepancies are usually apparent when there is more than three symbols, like the panels with 19 ply stringers in figure 7. (Data for panels that failed in the grips are not shown.) Strain measurements indicate that the stiffnesses of the two groups of like panels are equal. Thus, the discrepancies are probably not due to an error in layup.

MODIFICATIONS TO ACCOUNT FOR OUT-OF-PLANE EFFECTS

To account for out-of-plane effects, $(Et)_{st}$ in equation (3) was replaced by $(Et)_{st}e^{-\gamma\alpha}$ giving

$$\varepsilon_{tu}/\varepsilon_c = (\varepsilon_{tu}E_{sh}/K_Q)[(\varepsilon_{tu}E_{sh}/K_Q)^2+\frac{1}{2}\pi W_a/(1+\alpha e^{-\gamma\alpha})]^{1/2} \qquad (4)$$

The coefficient γ was determined to be 0.194 by fitting equation (4) to the data in figure (7) for panels with the thickest stringers of each sheet layup. The exponential factor was chosen because it is unity for small α and zero for large α. Predictions with equation (4) are shown in figure 8 along with the results in figure 7. Equations (3) and (4) give about the same results for the thinnest stringers. But, for thick stringers, equation (4) agrees with the data and gives much lower failing strains.

FAILING STRAIN VERSUS STRINGER SPACING

The failing strains are plotted against W_a in figure 9 for all the panels with a stringer stiffness ratio $\mu = 0.5$ and with arrested cracks. Values predicted with equation (4) are also plotted for comparison. The measured and predicted failing strains agree. The differences are within the scatter among like specimens.

The results in figures 7 - 9 indicate that, due to the out-of-plane effects, an increase in stringer thickness above the 9 or 15 plies does not result in much further increase in failing strain.

DESIGN CURVE FOR STIFFENED PANELS

It was shown in reference 4 that, when crack-tip damage is small, fracture toughness K_Q can be predicted with $K_Q = Q_c E_x/\xi$. The general fracture toughness parameter Q_c, in contrast to the fracture toughness K_Q, is independent of layup and varies only with ε_{tuf} the fiber failing strain. For laminates with little or no crack-tip damage, $Q_c = 0.30\varepsilon_{tuf}$ in.$^{1/2}$. The term $\xi = 1-\nu_{xy}(E_y/E_x)^{1/2}$

accounts for the effect of sheet layup. The ν_{xy}, E_x, and E_y are the elastic constants of the sheet, where x denotes the loading direction.

Substituting the above equation for K_Q into equation (4), recognizing that $E_x = E_{sh}$, and assuming that $\varepsilon_{tu} = \varepsilon_{tuf}$ gives

$$\varepsilon_c/\varepsilon_{tu} = 0.30[0.30^2+\tfrac{1}{2}\pi\xi^2 W_a/(1+\alpha e^{-\gamma\alpha})]^{-1/2} \qquad (5)$$

Equation (5) with $\gamma = 0.194$ is shown in figure 10 as a single design curve for stiffened panels with any sheet layup and made of any material. The $(45/0/-45/0)_{2S}$ data tend to be below the $(45/0/-45/90)_{2S}$ data because of crack-tip damage, which is not taken into account in the stress-intensity factor analysis. Crack-tip damage causes K_Q to be overpredicted for thin $(45/0/-45/0)_{2S}$ laminates and underpredicted for thin $(45/0/-45/90)_{2S}$ laminates (refs. 4 and 5). In comparison to scatter among like specimens, the agreement between the data and the design curve is good. A lower bound curve could be calculated using a value of $Q_c/\varepsilon_{tuf} < 0.30$ in.$^{1/2}$.

The curve in figure 10 does not indicate how wide a stringer must be. As noted previously, the shear-lag analysis indicates that the failing strains do not depend on stringer width W_{st}, as long as W_{st} is greater than some small value.

Without dynamic effects, the failing strains of panels without arrested cracks (short slots) should be above those with arrested cracks. The difference would be larger for shorter slots. Thus, the design curve in figure 10 would be a lower bound regardless of slot length or damage size. However, as noted previously, the test results indicate that the curve should be lowered slightly (less than 10 percent) to account for dynamic effects.

Also,as noted previously, thin stringers with a strong, stiff interface may fail first as the crack tip approaches. Likewise a weak adhesive may lead to very large disbonds. In both cases, panels could be weaker than the curve in figure 10 indicates. Additional work is needed to determine optimum stringer-interface properties.

MAXIMUM PREDICTED IMPROVEMENT WITH STRINGERS

Equations (4) and (5) predict a maximum increase in failing strain of stiffened panels over unstiffened panels. Calculations of the ratio of failing strain with stringers to that without stringers ($\alpha = 0$) using equation (5) are plotted against α in figure 11 for various values of W_a. The failing strain ratio has a maximum value at $\alpha = \alpha^*$, where $\alpha^* = 1/0.194$. The maximum value increases with $W_a$and asymptotically approaches 1.7. However, it is not very sensitive to $W_a$for $W_a > 1$ inch nor to α for $2 < \alpha < \alpha^*$. For the sheet layups

here, t_{st}/t_{sh} = 2.1 and 2.9 for $\alpha = \alpha^*$. Note that the curve in figure 11 without the out-of-plane correction indicates no limit in improvement.

OTHER STIFFENED PANEL DATA

Porter and Pierre (ref. 6) also measured the residual strength of graphite/epoxy panels with bonded one-inch-wide tear straps. (Panels with bolted tear straps were also tested and were found to have lower failing strains than like panels with bonded straps.) The panels were made with Fiberite T300/934 material, which is very similar to T300/5208. The tear straps were like the stringers in the present panels except they were located on both sides of the sheet, one opposite another, and they were made with a $(0/\pm45/90)_{NS}$ layup rather than a unidirectional layup. Thus, bending effects were minimum. The sheets were made with $(\pm45)_{4S}$ or $(0/\pm45/90)_{2S}$ layups. For the $(0/\pm45/90)_{2S}$ sheets, the straps were either 32 or 64 plies thick and were spaced either 4 or 6 in. on centers. For the $(\pm45)_{4S}$ sheets, the straps were 32 plies thick and spaced 4 in. on centers. Each panel had four straps, was 16 or 24 inches wide (depending on strap spacing), and contained a two-inch-long cut between the central two straps.

When the panels were loaded, cracks ran from the cuts and were arrested at the stringers like those in the present tests. The failing strains are plotted in figure 12 along with the present data and equation(5), the design curve. The graph is the same as that in figure 10 except that the data from reference 6 is plotted against $\xi^2 W_a/(1+\alpha)$, which assumes no bending effects. The data point from reference 6 with the arrow pointing up failed prematurely in the grips. The failing strains from reference 6 are significantly greater than the design curve, but are close to the largest failing strains of the present $(45/0/-45/90)_{2S}$ panels. As noted previously, crack-tip damage causes failing strains of thin $(45/0/-45/90)_{2S}$ and thin $(0/\pm45/90)_{2S}$ laminates to be underpredicted.

Values of Q_c for the same laminates without stringers or straps are plotted in figure 13 against crack length. Values for $(45/0/-45/90)_{2S}$ T300/BP-907 are also plotted for comparison. (The BP-907 epoxy is made by American Cyanamid Company.) The T300/934 data is from reference 6 and the T300/5208 and T300/BP-907 data are from reference 7. The general fracture toughness parameter Q_c is proportional to K_Q and should be independent of layup and matrix when crack-tip damage is small (ref.7). The values of Q_c increase significantly with crack length 2a for the 934 and 5208 epoxies but not for BP-907 (at least not for crack lengths up to 1.6 in.). The BP-907 is much stronger and tougher than 934 and 5208 and results in much less crack-tip damage. The value of Q_c for the 934 specimen is 0.0042 $in.^{1/2}$. The design curve for Q_c = 0.0042 $in.^{1/2}$ is also plotted in figure 12 to allow for crack-tip damage. The design curve for Q_c =

0.0042 in.$^{1/2}$ is considerably higher than that for Q_c = 0.0030 in.$^{1/2}$, but it is still below the data from reference 6 by as much as 23 percent.

Because the present panels and those from reference 6 had different configurations, direct comparisons of failing strains cannot be made to show the effect of bending. However, the ratio of failing strains with and without bending can be predicted with equation (5) by assuming $\gamma = 0$ for no bending and $\gamma = 0.194$ for bending. For the $(0/\pm45/90)_{2S}$ T300/934 panels, the largest predicted ratio of failing strains is 1.3, and, for the $(45/0/-45/90)_{2S}$ T300/5208 panels, the largest predicted ratio is 1.6. Thus, panels with straps or stringers on both sides of the sheet should be significantly stronger than panels with straps or stringers on only one side. Therefore, the application of test results for panels with straps or stringers on both sides to structures with straps or stringers on only one side would be very unconservative.

CONCLUSIONS

1. Bonded stringers can arrest cracks and increase failing strains of graphite/epoxy panels.

2. Failing strains increase with the thickness, Young's modulus, and spacing of stringers.

3. In contrast to riveted or bolted stringers, the area (or width) of bonded stringers may be relatively unimportant.

4. With stringers on one side of the sheet, bending limits the increase in failing strain with stringer thickness and Young's modulus to 70 percent of that without stringers.

5. With bending, the increase in failing strain is a maximum when the thickness of unidirectional stringers is 2 or 3 times that of $(45/0/-45/90)_{2S}$ or $(45/0/-45/0)_{2S}$ sheets, respectively.

6. With stringers located symmetrically on both sides of the sheet, bending is minimum, and failing strains of panels can be much larger than those of like panels with stringers only on one side.

7. A fracture mechanics analysis predicts the failing strains well.

8. A single design curve was developed using the analysis and the fracture toughness parameter Q_c.

REFERENCES

1. Arin, K.: A Plate with a Crack, Stiffened by a Partially Debonded Stringer. Engineering Fracture Mechanics, 1974, Vol. 6, pp. 133-140.

2. Poe, Jr. C. C.: Stress-Intensity Factor for a Cracked Sheet with Riveted and Uniformly Spaced Stringers. NASA TR R-358, May 1971.

3. Kennedy, J. M.: Fracture Behavior of Hybrid Composite Laminates. AIAA/ASME/ASCE/AHS 24th Structures, Structural Dynamics and Materials Conference. Lake Tahoe, NV, May 2-4, 1983.

4. Poe, Jr., C. C.: A Unifying Strain Criterion for Fracture of Fibrous Composite Laminates. Engineering Fracture Mechanics, Vol. 17, No. 2, pp. 153-171, 1983.

5. Harris, C. E.; and Morris, D. H.: Fracture Behavior of Thick, Laminated Graphite/Epoxy Composites. NASA CR-3784, 1984.

6. Porter, T. R.; and Pierre, W. F.: Tear Strap Design in Graphite/Epoxy Structure. Proceedings - Fifth DOD/NASA Conference on Fibrous Composites in Structural Design - Vol. II, New Orleans, LA, Jan. 27-29, 1981, pp. 265-280.

7. Poe, Jr. C. C.: Fracture Toughness of Fibrous Composite Materials. NASA TP 2370, 1984.

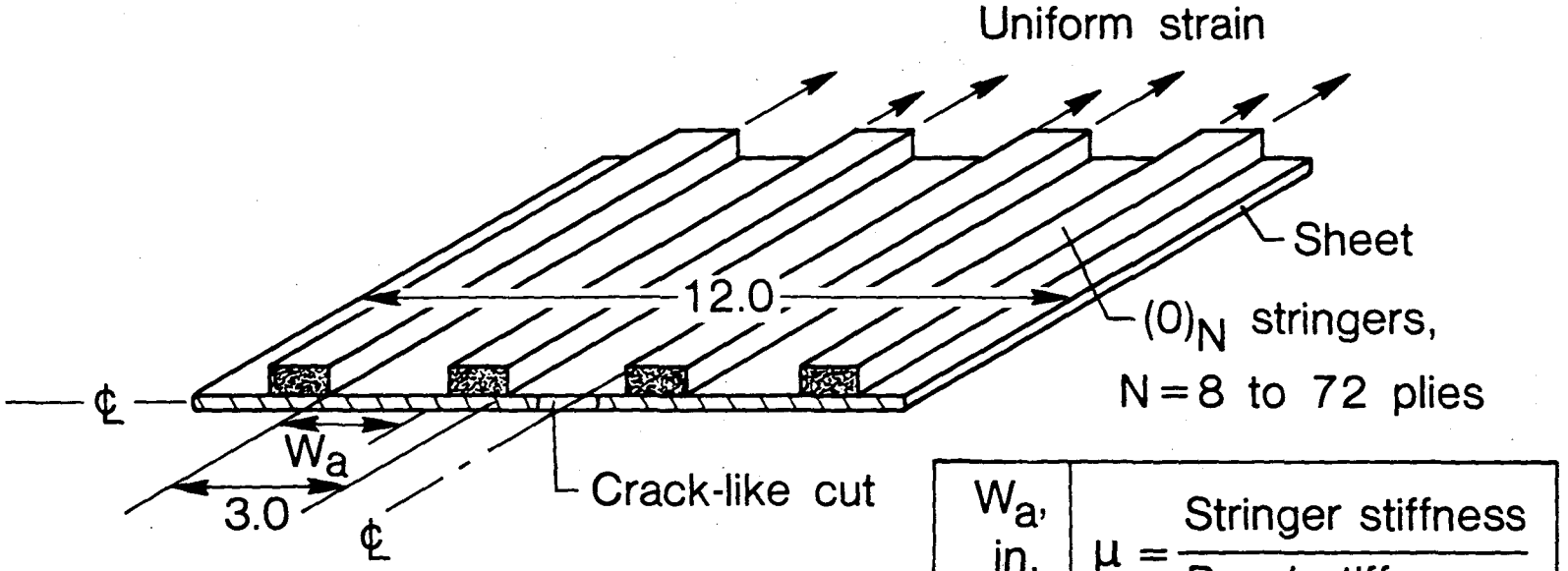

Material: T300/5208

Sheet layups: $(45/0/-45/90)_{2S}$ and $(45/0/-45/0)_{2S}$

W_a, in.	$\mu = \frac{\text{Stringer stiffness}}{\text{Panel stiffness}}$
2.0	0.3
.5 2.0 2.5	.5
2.0	.7

Figure 1. - Configuration of stiffened panels.

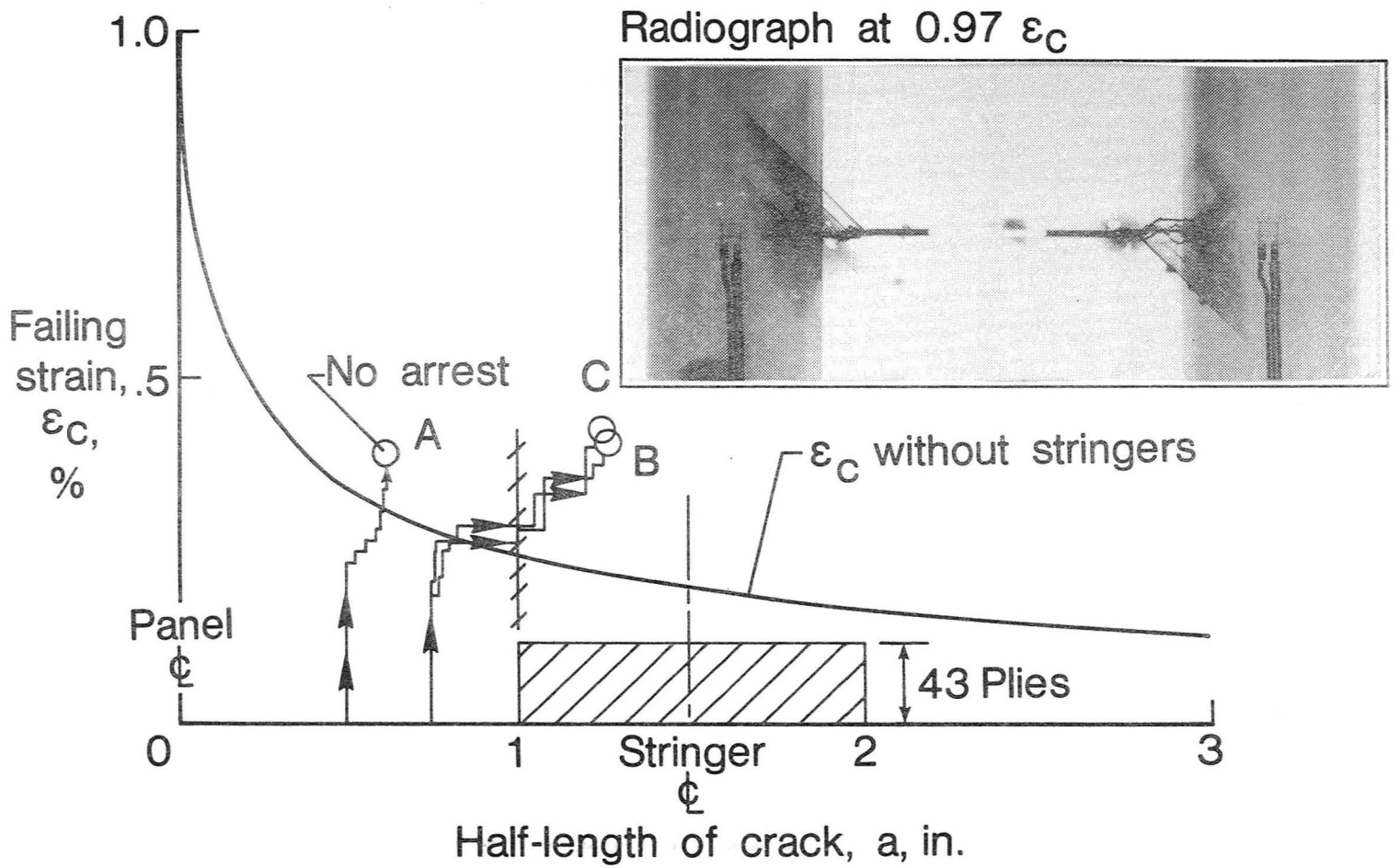

Figure 2. - Test results for $(45/0/-45/90)_{2s}$ panels with $\mu = 0.7$.

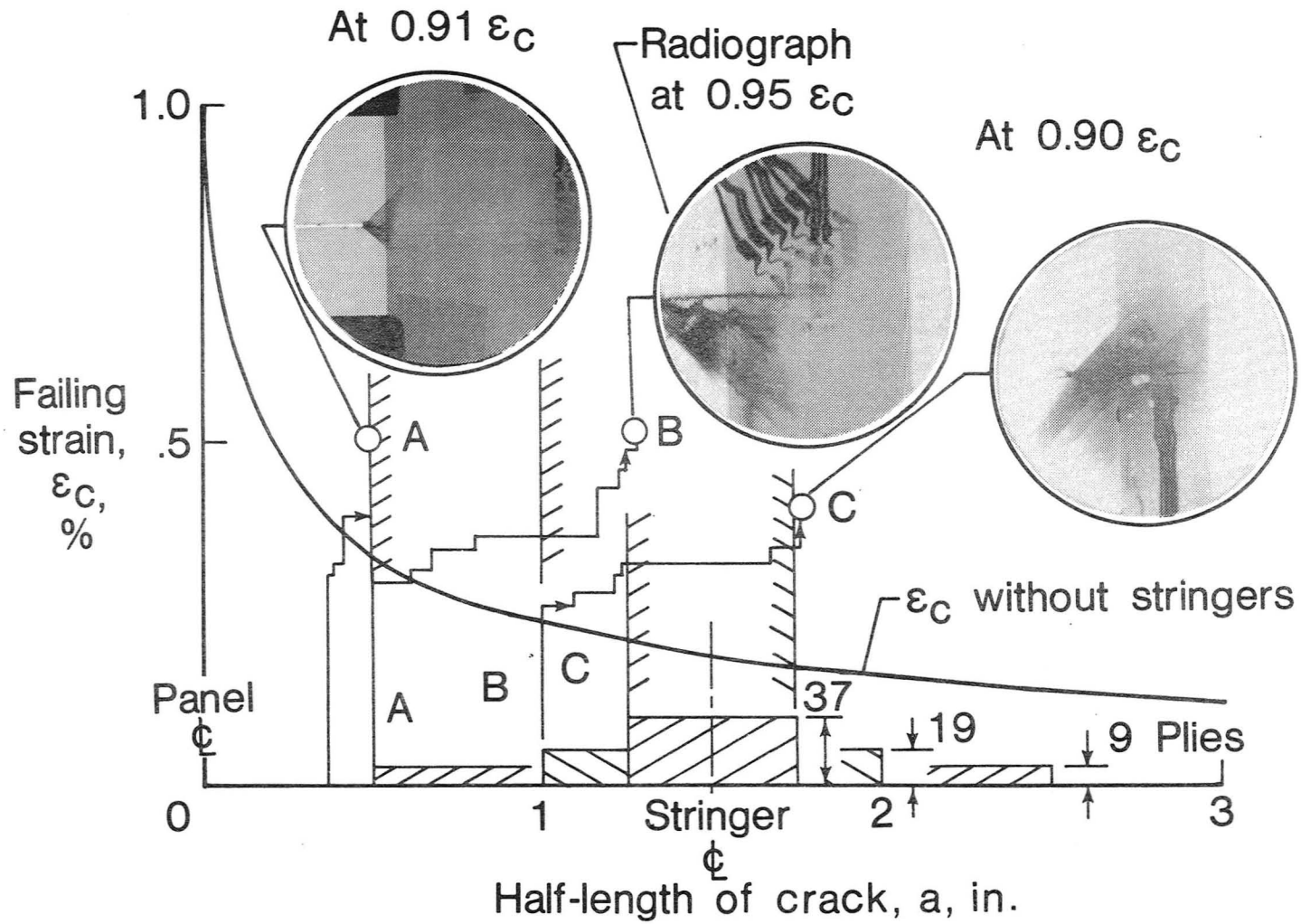

Figure 3. - Test results for $(45/0/-45/90)_{2s}$ panel with $\mu = 0.5$.

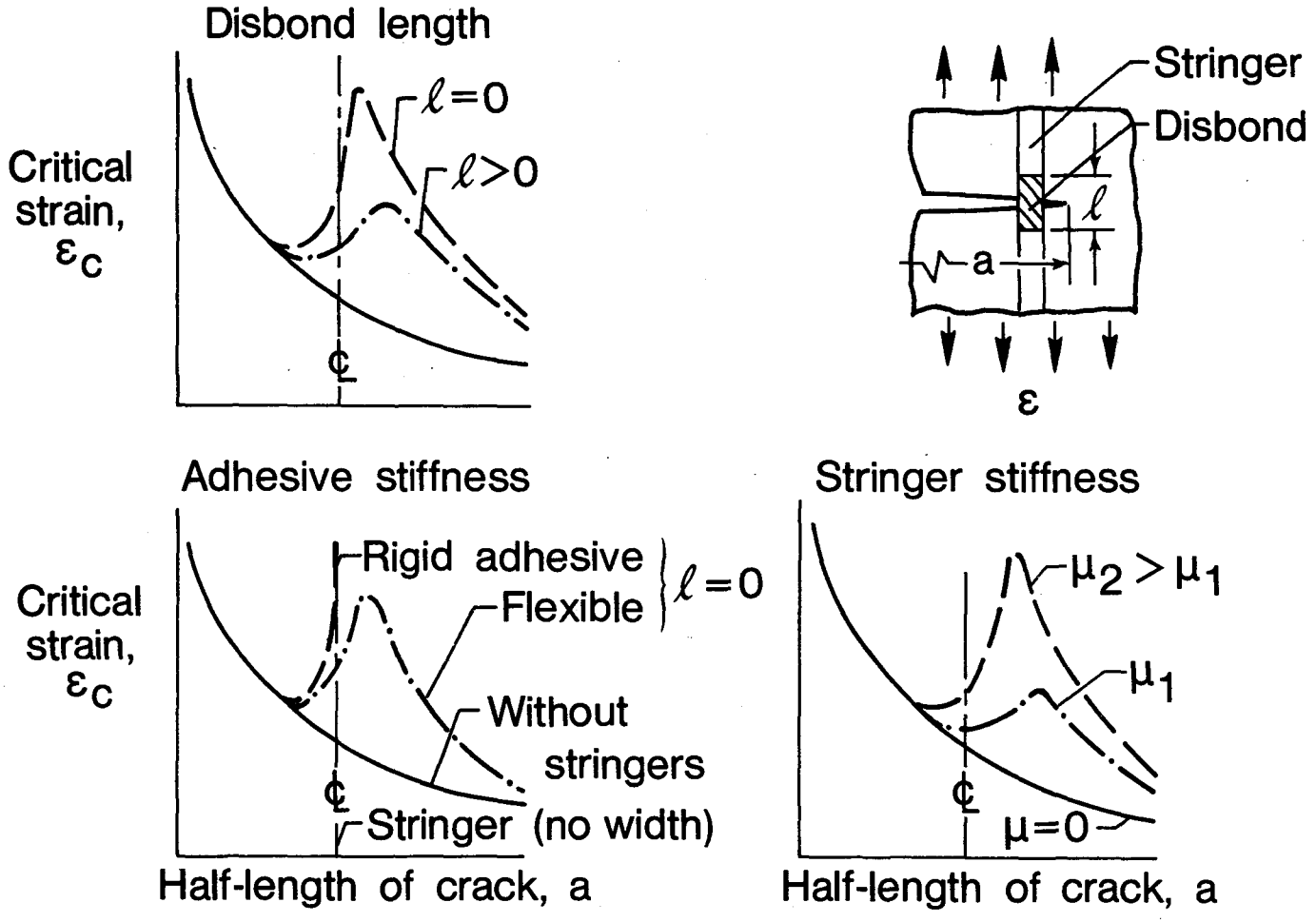

Figure 4. - Analysis for bonded stringers.

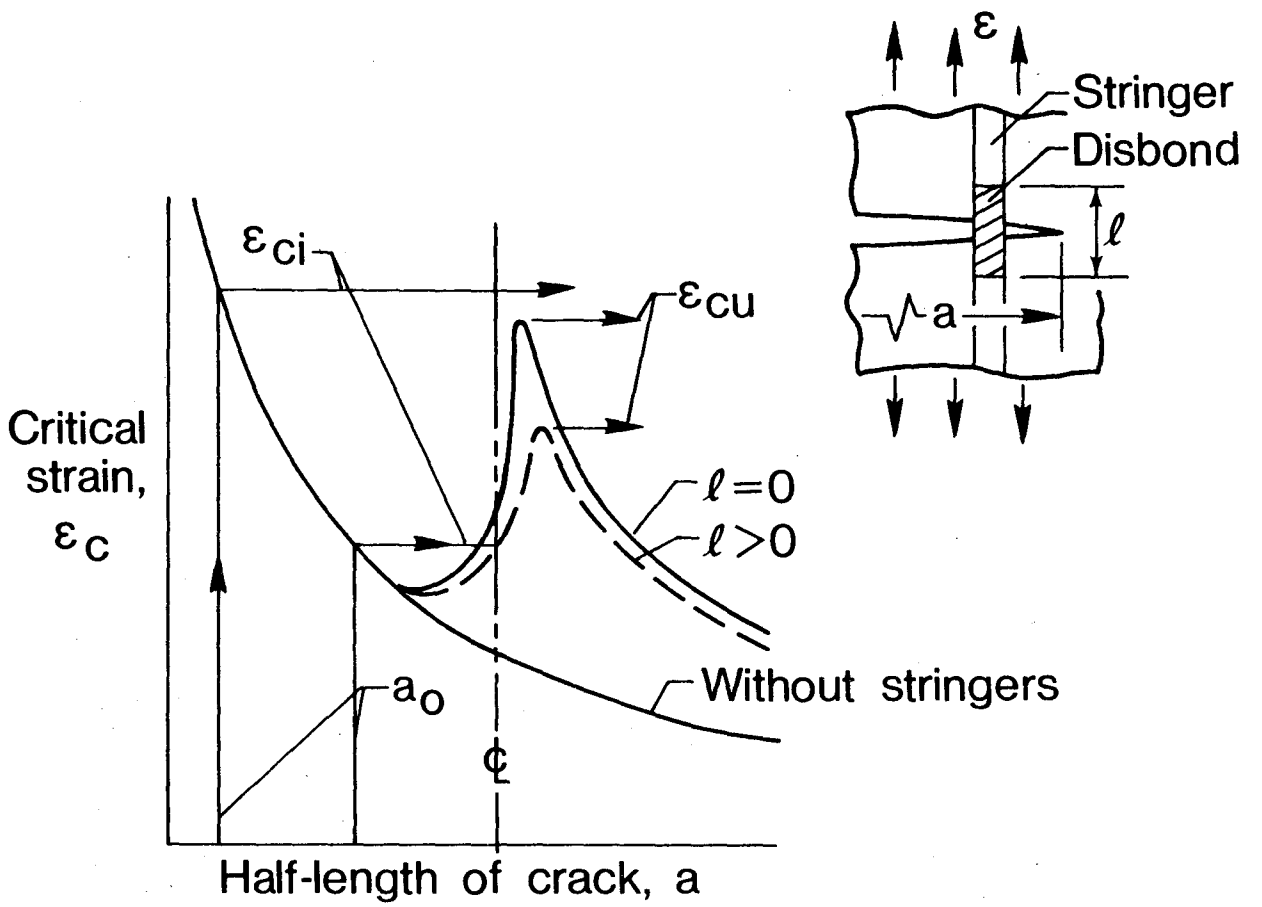

Figure 5. - Predicting failing strains.

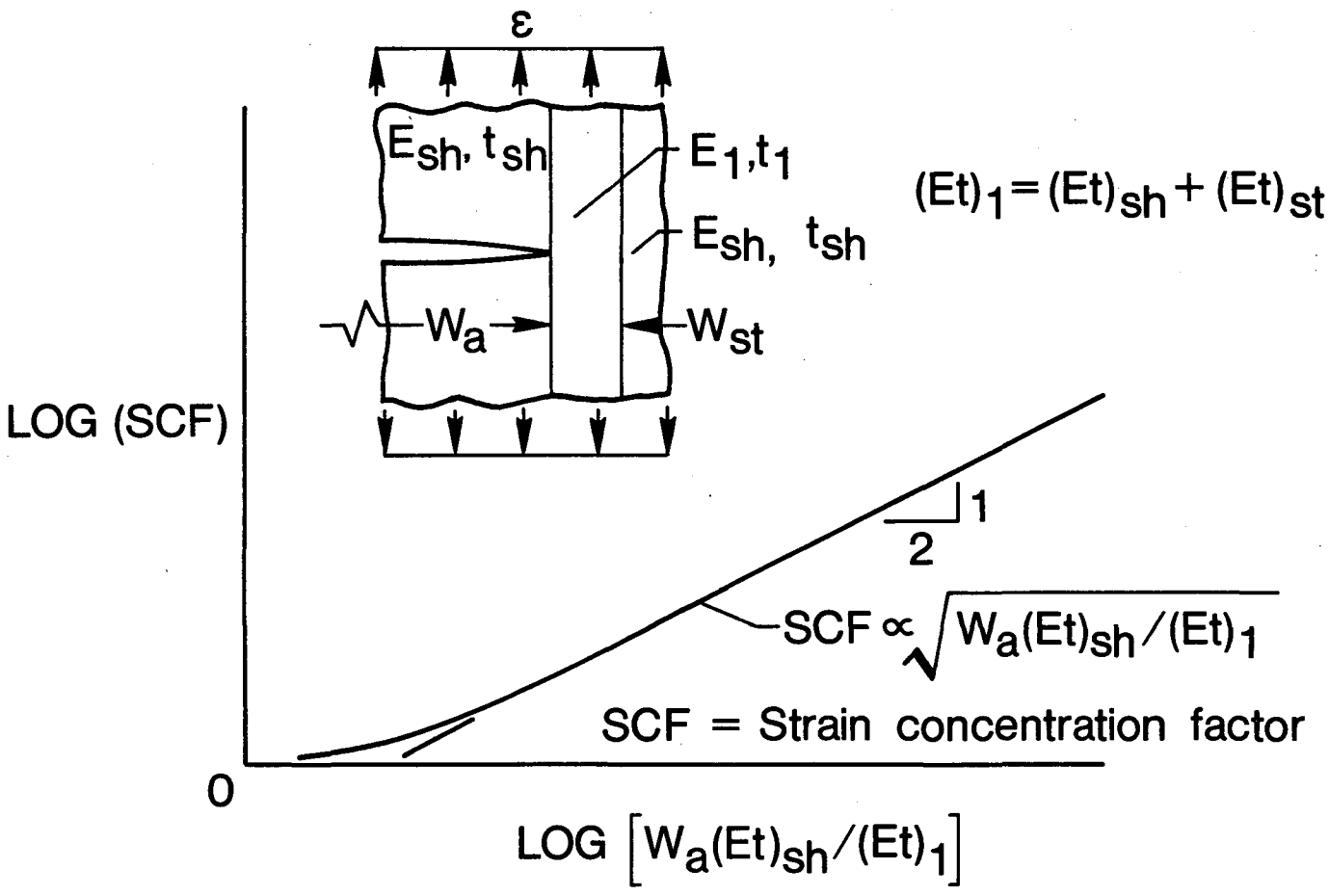

Figure 6. - Shear-lag analysis.

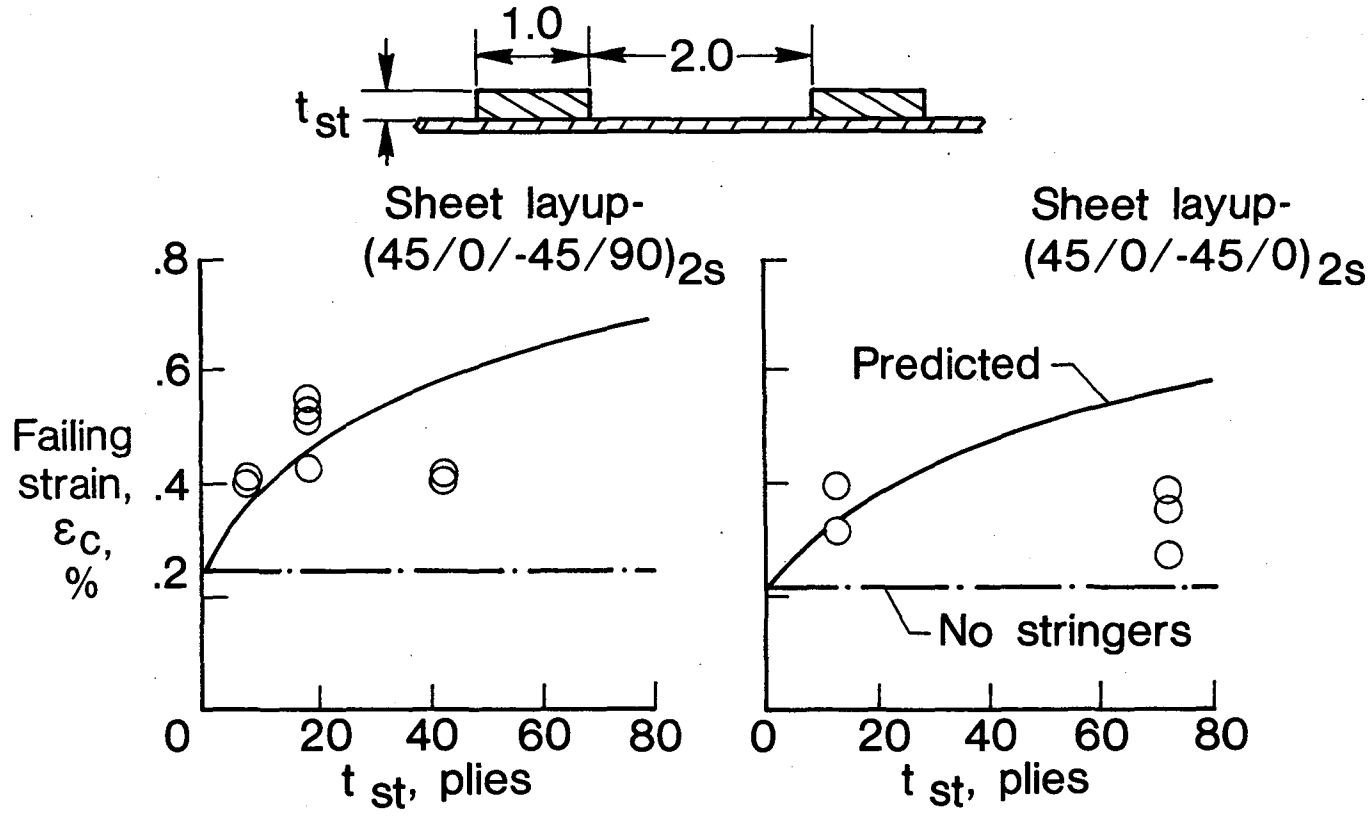

Figure 7. - Failing strain versus stringer thickness.

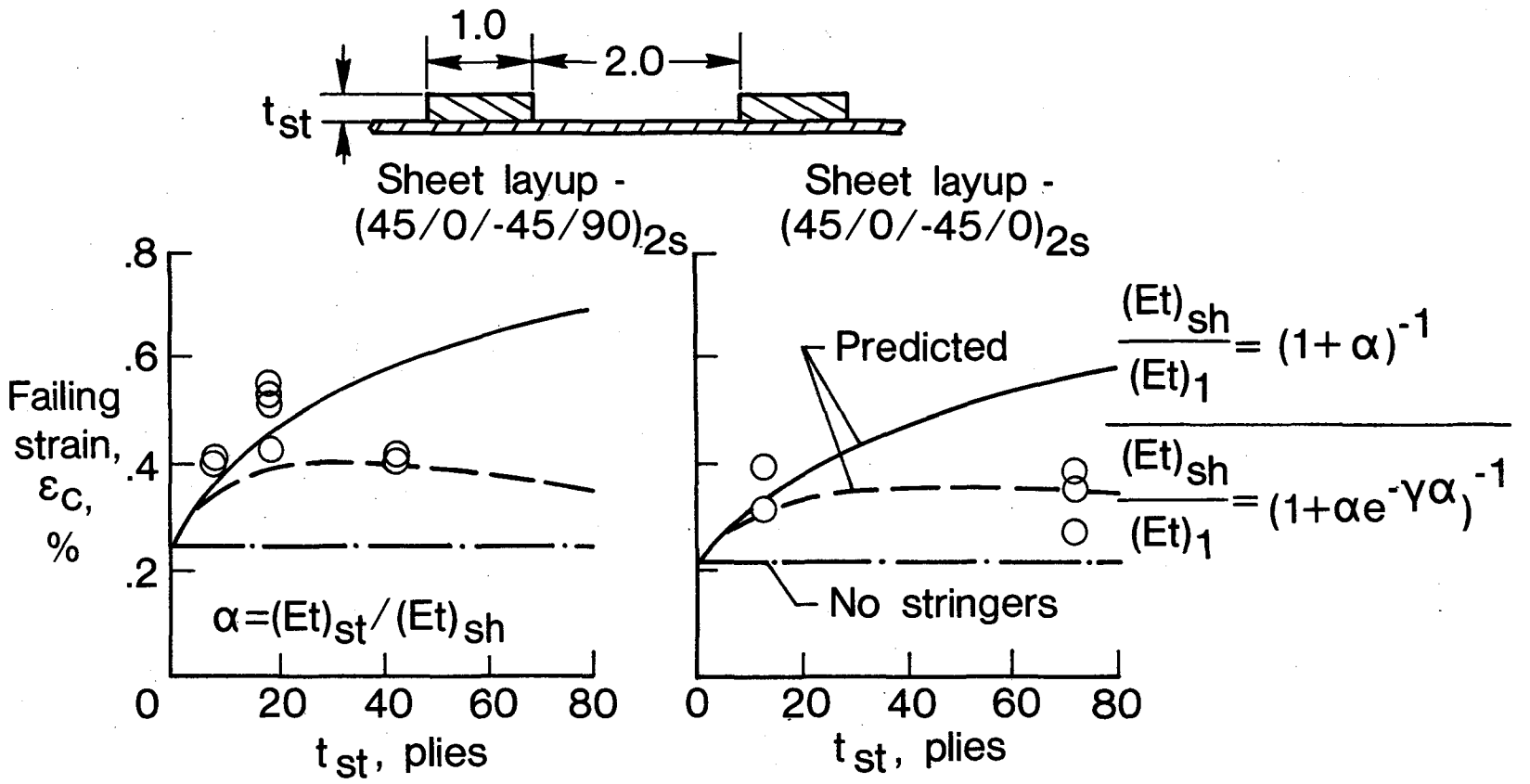

Figure 8. - Failing strain versus stringer thickness with predictions modified for out-of-plane effects.

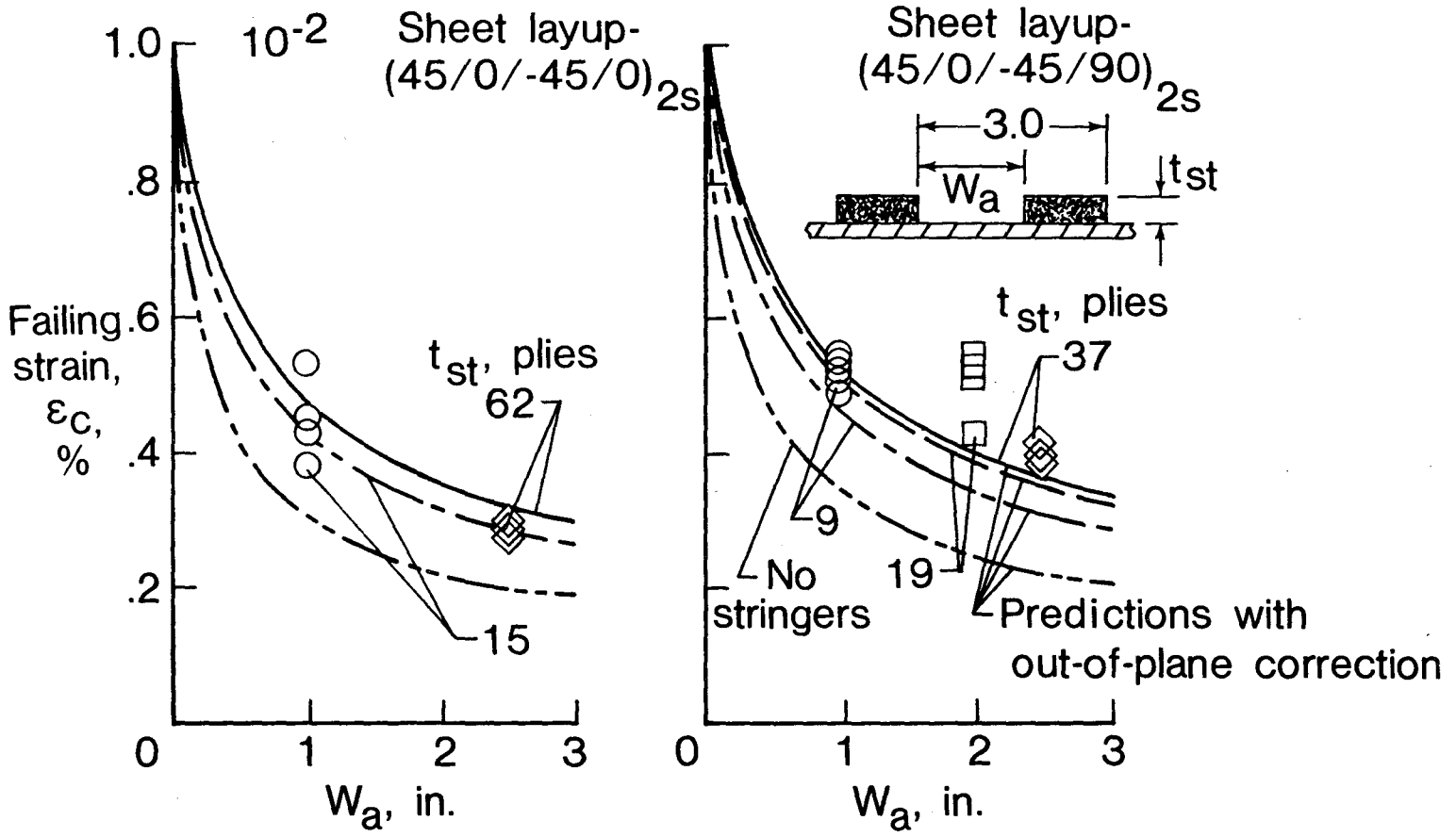

Figure 9. - Failing strain versus stringer spacing for $\mu = 0.5$.

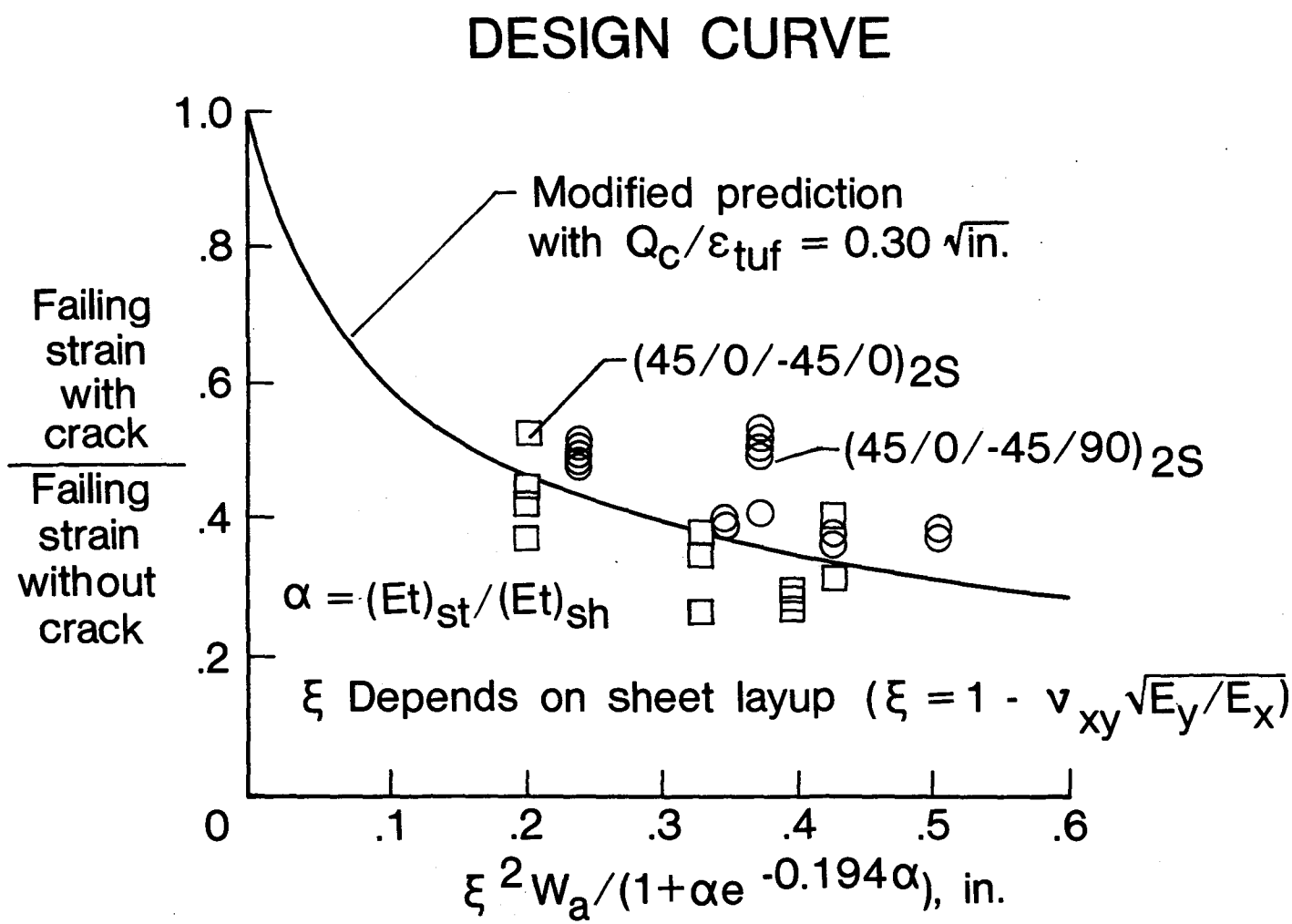

Figure 10. - Design Curve.

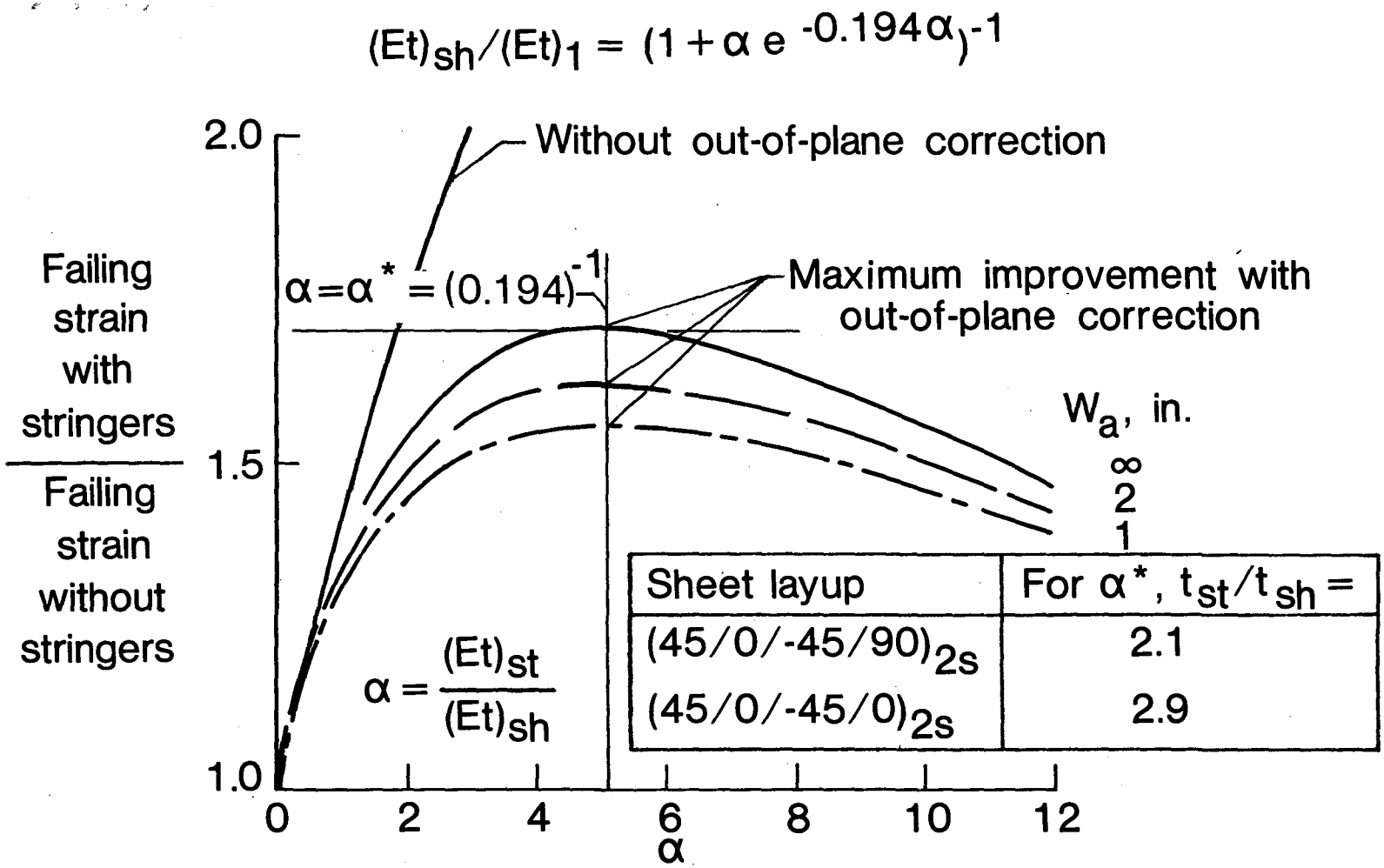

Figure 11. - Maximum predicted improvement with stringers.

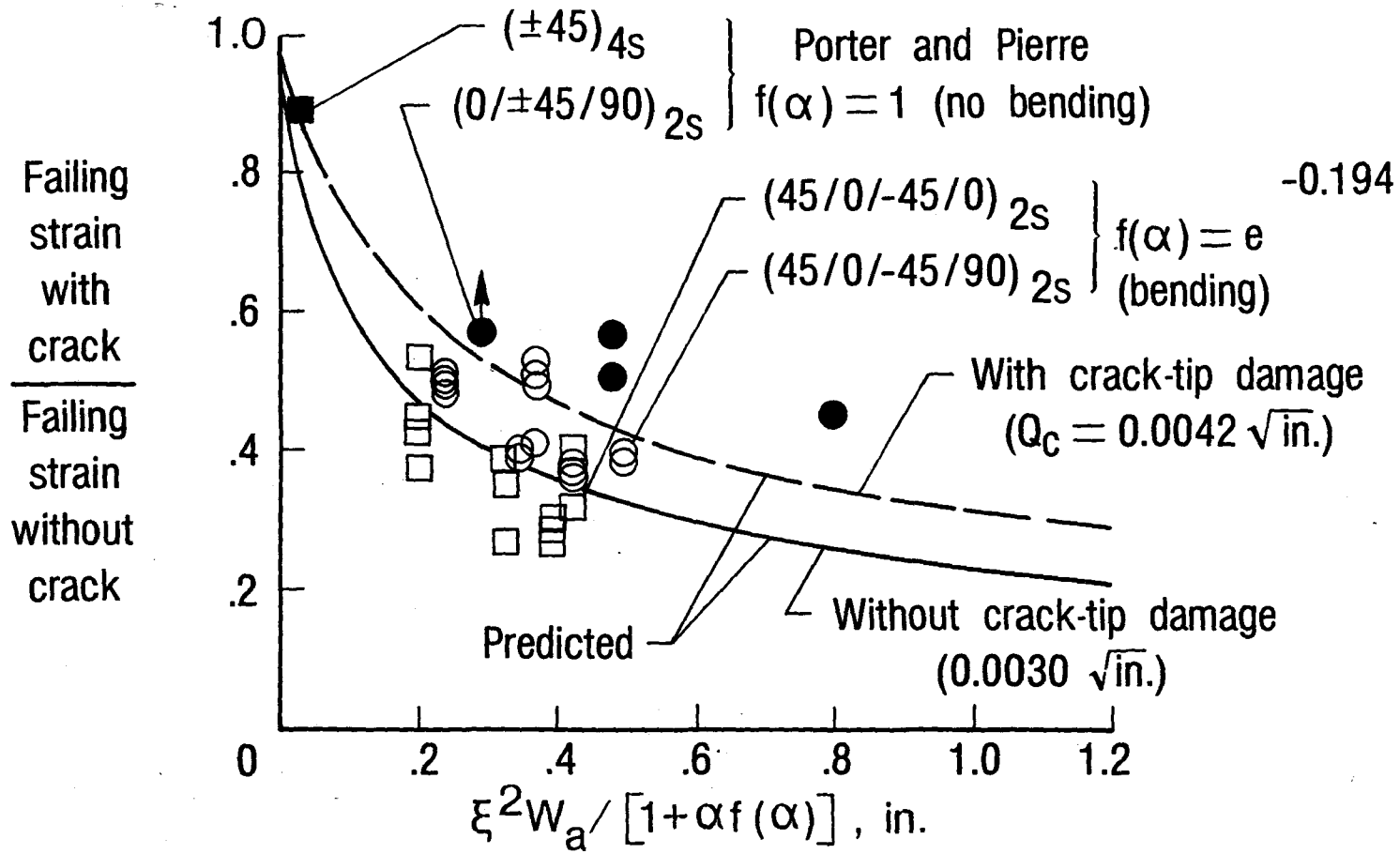

Figure 12. - Comparison with stiffened panel data of Porter and Pierre.

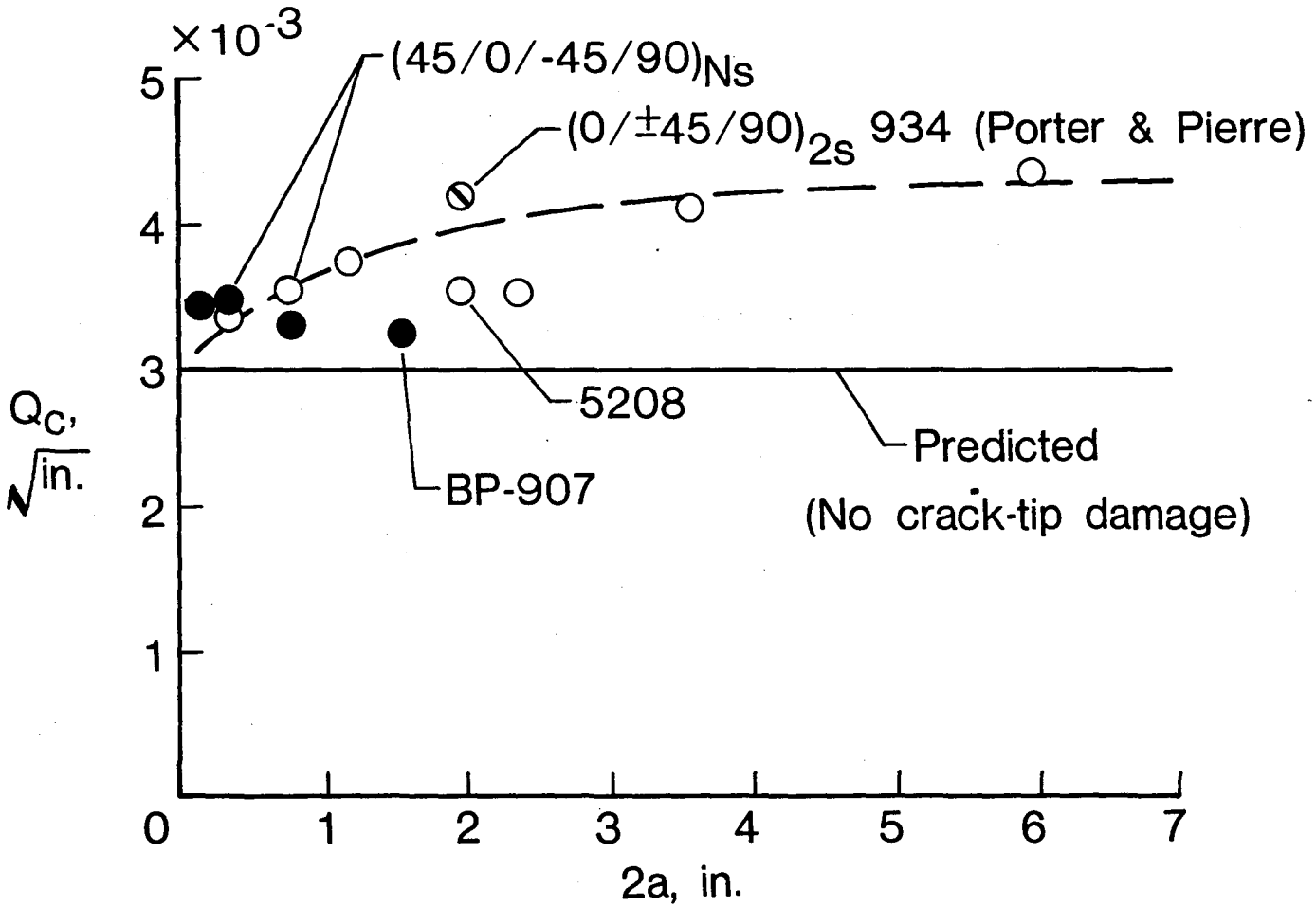

Figure 13. - Toughness and crack size. T300/epoxy.

1. Report No.	2. Government Accession No.	3. Recipient's Catalog No.
NASA TM-86310		

4. Title and Subtitle	5. Report Date
Tensile Strength of Composite Sheets With Unidirectional Stringers and Crack-Like Damage - A Brief Report	September 1984
	6. Performing Organization Code: 506-33-23-05

7. Author(s)	8. Performing Organization Report No.
C. C. Poe, Jr.	
	10. Work Unit No.
9. Performing Organization Name and Address	
NASA Langley Research Center Hampton, VA 23665	11. Contract or Grant No.
	13. Type of Report and Period Covered: Technical Memoranudm
12. Sponsoring Agency Name and Address	
National Aeronautics and Space Administration Washington, DC 20546	14. Sponsoring Agency Code

15. Supplementary Notes

16. Abstract

The purpose of this investigation was to determine the residual strength of composite sheets with bonded composite stringers loaded in tension. This report summarizes the results.

About 50 graphite/epoxy composite panels with crack-like slots were monotonically loaded in tension to failure. Both sheet layup and stringer configuration were varied. The tests indicate that the composite panels have considerable damage tolerance. The stringers arrested cracks that ran from the crack-like slots, and the residual strengths were considerably greater than those of unstiffened composite sheets.

A stress-intensity factor analysis was developed to predict the failing strains of the stiffened panels. Using the analysis, a single design curve was produced for composite sheets with bonded stringers of any configuration.

17. Key Words (Suggested by Author(s))	18. Distribution Statement
fracture, composites, stringers, tensile strength	Unclassified - Unlimited Subject Category 24

19. Security Classif. (of this report)	20. Security Classif. (of this page)	21. No. of Pages	22. Price
Unclassified	Unclassified	26	A03

N-305

For sale by the National Technical Information Service, Springfield, Virginia 22161